Dimensional Analysis of the Earthquake Response of a Pounding Oscillator

Elias Dimitrakopoulos[1]; Nicos Makris, M.ASCE[2]; and Andreas J. Kappos[3]

Abstract: In this paper, the dynamic response of a pounding oscillator subjected to pulse type excitations is revisited with dimensional analysis. The study adopts the concept of the energetic length scale which is a measure of the persistence of the distinguishable pulse of strong ground motions and subsequently presents the dimensionless Π products that govern the response of the pounding oscillator. The introduction of Buckingham's Π theorem reduces the number of variables that govern the response of the system from 7 to 5. The proposed dimensionless Π products are liberated from the response of an oscillator without impact and most importantly reveal remarkable order in the response. It is shown that, regardless the acceleration level and duration of the pulse, all response spectra become self-similar and, when expressed in the dimensionless Π products, follow a single master curve. This is true despite the realization of contacts with increasing durations as the excitation level increases. All physically realizable contacts (impacts, continuous contacts, and detachment) are captured via a linear complementarity approach. The proposed analysis stresses the appreciable differences in the response due to the directivity of the excitation (toward or away the stationary wall) and confirms the existence of three spectral regions where the response of the pounding oscillator amplifies, deamplifies, and equals the response of the oscillator without pounding.

DOI: 10.1061/(ASCE)0733-9399(2010)136:3(299)

CE Database subject headings: Dimensional analysis; Earthquake engineering; Oscillations.

Author keywords: Pounding; Dimensional analysis; Earthquake engineering; Unilateral contact.

Introduction

A major challenge in studying the response of pounding structures is no longer the dynamic response analysis of a specific configuration but rather the presentation of the response analysis in a way that is most meaningful for a wide class of structural configurations. This challenge emerged partly because (1) of a wide variety and a large number of parameters that govern the response of pounding structures; (2) an ever increasing database of recorded ground motions with quite complex patterns; and (3) several conflicting conclusions published in the literature.

Despite its apparent simplicity, the structural configuration of a single-degree-of-freedom (SDOF) system pounding against a stationary monolithic wall, called pounding (or impact) oscillator, presents a rich nonlinear dynamic behavior including subharmonic resonances and bifurcation branches which may lead to chaotic behavior (Thompson and Stewart 2001). Analytical studies on the response of the impact oscillator have been presented by Wolf and Skrikerud (1980); Shaw and Holmes (1983); and Davis (1992) among others, focusing mainly on its steady-state response under harmonic excitation. Wolf and Skrikerud unveiled on the subharmonic resonances that emerge due to repeated poundings under harmonic excitation, while Shaw and Holmes examined the same problem within the context of "dynamical systems" and investigated the bifurcations in the behavior of the impact oscillator. Davis identified spectral areas with periodic, nonperiodic as well as chaotic contacts, while he elaborated on the directivity of the pulse and the influence of the gap that was normalized with respect to the peak ground displacement. Several researchers have studied the response of two or more colliding SDOF systems, as well as the response of adjacent buildings or bridge segments due to earthquake shaking [e.g., see references reported in DesRoches and Muthukumar (2002)].

This paper revisits the problem of pounding of a SDOF system against a stationary monolithic wall due to earthquake shaking with the aid of formal dimensional analysis (Langhaar 1951; Sedov 1959; Barenblatt 1996). Its aim is to offer an alternative, yet most natural, way to present the response of a pounding oscillator which is liberated from the response of the oscillator without pounding and makes use of the fundamental concept of self-similarity, a special type of symmetry which is invariant with respect to size transformations. The application of the proposed method hinges upon the existence of a distinct time scale and a length scale that characterize the most energetic component of ground shaking. Such time and length scales emerge naturally from the distinguishable pulses which dominate a wide class of strong earthquake records; they are directly related with the rise time and slip velocity of faulting and can be formally extracted with validated mathematical models available in the literature.

Mathematical Formulations on Impact and Contact

The behavior of a dynamical system with unilateral contact can be expressed through the equation of Pfeiffer and Glocker (1996)

[1]Doctoral Candidate, Dept. of Civil Engineering, Aristotle Univ. of Thessaloniki, Thessaloniki GR 54124, Greece.

[2]Professor, Dept. of Civil Engineering, Univ. of Patras, Patras GR 26500, Greece (corresponding author). E-mail: nmakris@upatras.gr

[3]Professor, Dept. of Civil Engineering, Aristotle Univ. of Thessaloniki, Thessaloniki GR 54124, Greece.

Note. This manuscript was submitted on January 17, 2008; approved on September 21, 2009; published online on February 12, 2010. Discussion period open until August 1, 2010; separate discussions must be submitted for individual papers. This paper is part of the ***Journal of Engineering Mechanics***, Vol. 136, No. 3, March 1, 2010. ©ASCE, ISSN 0733-9399/2010/3-299–310/$25.00.

$$\mathbf{M} \cdot \dot{\mathbf{q}} - \mathbf{h}(t, \mathbf{q}, \dot{\mathbf{q}}) - \mathbf{W} \cdot \boldsymbol{\lambda} = 0 \quad (1)$$

where $\mathbf{M}$=mass matrix; $\mathbf{W}$=direction vector of the constraint contact force; $\boldsymbol{\lambda}$=Lagrange multiplier; $\mathbf{q}$=generalized coordinates vector; and $\mathbf{h}$=vector of the nonimpulsive forces.

The basic assumptions of this method (Pfeiffer and Glocker 1996) are, in essence, those of rigid bodies, i.e., (1) impact is assumed to be "very short," yet separable into two phases, the compression phase (begins at time instant t_A when contact is initiated and terminates at t_C when the approaching process is completed) and the expansion phase (initiates at time t_C and terminates at t_E with the separation of the contacting bodies); (2) during impact, all magnitudes of the system (position, orientation, nonimpulsive forces) remain constant; (3) wave propagation effects generated by collision are neglected.

All physically feasible unilateral contact configurations (impacts, continuous contacts, and detachments) are mathematically treated as inequality problems, namely, linear complementarity problems (LCPs) (Pfeiffer and Glocker 1996; Brogliato 1999). In the classical form, a LCP is a system of linear equations: $\mathbf{y}=\mathbf{A}\mathbf{x}+\mathbf{b}$, with matrices $\mathbf{A}$ and $\mathbf{b}$ known, and $\mathbf{y}$ and $\mathbf{x}$ the unknown vectors under determination, for which the following additional complementarity conditions hold: $\mathbf{y} \geq 0$, $\mathbf{x} \geq 0$, $\mathbf{y}^T\mathbf{x}=0$.

According to Leine et al. (2003), two similar LCPs are formulated at the velocity level to capture the velocity jumps associated with the two impact phases (compression and expansion) and one additional LCP is formulated at the acceleration level for the treatment of continuous contacts and detachment. In the following, the aforementioned LCPs are presented in a simplified version since in the present study, contact is assumed to be frictionless and centric.

Continuous Contact and Detachment

Assuming the impenetrability constraint of the contact surface holds, then the relative distance in the normal (to the contact surface) direction of a contact, g_N, must always satisfy the inequality constraint: $g_N \geq 0$. Every time the normal distance vanishes, $g_N(t)=0$, contact takes place. With respect to the normal direction of a contact, there are two types of contacts: the instantaneous (impacts) and the continuous (finite duration) contacts which appear when additionally the relative velocity of the contacting bodies, $\dot{g}_N(t)=0$, vanishes. This can be either due to totally plastic impact, or successive inelastic impacts. A continuous contact results in a contact force, λ, which can be calculated as a Lagrange multiplier that must satisfy the constraint: $\lambda \geq 0$ due to the unilateral character of a contact. Otherwise, if $\lambda < 0$ the contact force lacks physical interpretation and therefore the time instant when the contact force changes sign (from positive to negative) is interpreted as the instant of detachment—separation of bodies (end of a contact). This contact force, λ, which is a scalar quantity in the simple case examined herein, can be determined from a LCP formulated at the acceleration level as (Leine et al. 2003)

$$\ddot{g}_N = W^T M^{-1} h + W^T M^{-1} W \lambda, \quad \ddot{g}_N \geq 0, \quad \lambda \geq 0, \quad \ddot{g}_N \cdot \lambda = 0 \quad (2)$$

Impact-Compression Phase

At the end of the compression phase, the relative velocity, $\dot{g}_{NC}$, and the impulse, Λ_{NC}, in the normal direction of the contact form a LCP which can be written as

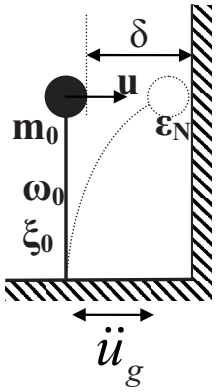

Fig. 1. Configuration of pounding oscillator subjected to ground motions

$$\dot{g}_{NC} = W^T M^{-1} W \Lambda_{NC} + \dot{g}_{NA}, \quad \dot{g}_{NC} \geq 0, \quad \Lambda_{NC} \geq 0, \quad \dot{g}_{NC} \cdot \Lambda_{NC} = 0 \quad (3)$$

where subindex N stands for the normal direction of contact; subindices C, E, and A stand for compression, expansion [see Eq. (4)] phase, and the time instant contact begins, respectively; and Λ stands for impulse of contact.

Impact-Expansion Phase

Similarly, the relative velocity at the end of the expansion phase, $\dot{g}_{NC}$, forms a LCP with the impulse, $\Lambda_{NP}=\Lambda_{NE}-\varepsilon_N\Lambda_{NC}$, which can be written as

$$\dot{g}_{NE} = (W^T M^{-1} W)\Lambda_{NP} + W^T M^{-1} W \varepsilon_N \Lambda_{NC} + \dot{g}_{NC}, \quad \dot{g}_{NE} \geq 0, \quad \Lambda_{NE} \geq 0, \quad \dot{g}_{NE} \cdot \Lambda_{NE} = 0 \quad (4)$$

The contact law used in the present study is that of Poisson's, according to which the coefficient of restitution, ε_N, is the impulse ratio of the approach and expansion phases. It is reminded that Newton's coefficient of restitution is taken as the ratio of the (relative) contact velocities after, $\dot{g}_{NE}$, and before, $\dot{g}_{NA}$, impact: $\dot{g}_{NE}=-\varepsilon_N\dot{g}_{NA}$. However, for the particular case of the pounding oscillator, which is a single-contact configuration, Poisson's and Newton's laws for impact are equivalent (Pfeiffer and Glocker 1996).

Time Scales and Length Scales in Strong Earthquake Records

One of the novelties of this work is that the response of the pounding oscillator (Fig. 1) is normalized to a measure of the persistence of the excitation—a length scale of the energetic component of the ground shaking. During the last three decades an ever increasing database of recorded ground motions has shown that the kinematic characteristics of the ground motion near the fault of major earthquakes contains distinguishable velocity and displacement pulses. The relatively simple form, yet destructive potential of near source ground motions, has motivated the development of various closed-form expressions which approximate their leading kinematic characteristics. The early work of Veletsos et al. (1965) was followed by those of Hall et al. (1995); Heaton et al. (1995); Makris (1997); Makris and Chang (2000); Alavi and Krawinkler (2001); Mavroeidis and Papageorgiou (2003); and Makris and Black (2004c). Some of the proposed pulses are

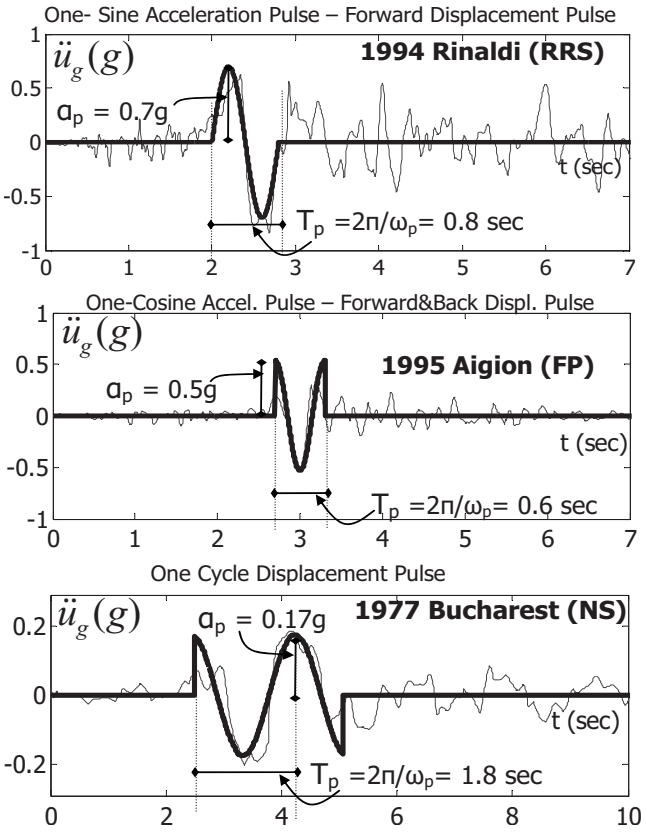

Fig. 2. Earthquake records with distinguishable acceleration pulse

physically realizable motions with zero final ground velocity and finite accelerations, whereas some other approximations violate one or both the above requirements. Physically realizable trigonometric pulses can adequately describe the impulsive character of near-fault ground motions both qualitatively and quantitatively. The input parameters of the model have an unambiguous physical meaning. The minimum number of parameters is 2, which are either their acceleration amplitude, α_p, and duration, T_p, or the velocity amplitude, v_p, and duration, T_p. Fig. 2 plots the time histories of the Rinaldi station record, from the 1994 Northridge earthquake, the Greek Organization of Telecommunications record from the 1995 Aegion earthquake and the Bucharest record of the 1977 Vrancea earthquake are also shown. In all three records the pulse duration, T_p, and the pulse acceleration, α_p, are shown. It is worth mentioning that the distinguishable pulse in the Bucharest record is due to the presence of a deposit that filtered/amplified an earthquake signal which was generated more than 160 km away.

The more sophisticated model of Mavroeidis and Papageorgiou (2003) involves four parameters, which are the pulse period and the pulse amplitude as well as the number and phase of half-cycles, and was found to describe a large set of velocity pulses generated due to forward directivity of strong ground motions. The pulse period, T_p, of the most energetic pulse is strongly correlated with the moment magnitude, M_w, of the event (Hall et al. 1995; Papageorgiou and Aki 1983; Mavroeidis and Papageorgiou 2003). Furthermore, seismological data indicate that the amplitude of the velocity pulses recorded within a distance of 7 km from the causative fault varies from 70 to 130 cm/s. This observation is in good agreement with the typical slip velocity of 100 cm/s frequently considered by seismologists (Brune 1970; Aki 1983).

The current established methodologies for estimating the pulse characteristics of a wide class of records are of unique value since the product $\alpha_p T_p^2 \sim L_e$ is a characteristic length scale of the ground excitation and is a measure of the persistence of the most energetic pulse to generate inelastic deformations, in the case of yielding oscillators (Makris and Black 2004a,b; Makris and Psychogios 2006). The reader should recall that among two pulses with different acceleration amplitude (say $\alpha_{p1} > \alpha_{p2}$) and different pulse duration (say $T_{p1} < T_{p2}$), the deformation demands (and eventually impacts and finite duration contacts) do not scale with the peak pulse acceleration (most intense pulse) but with the stronger length scale (larger $\alpha_p T_p^2$ gives the most persistent pulse).

Elastic SDOF Oscillator with Unilateral Contact Subjected to Base Excitation

In the particular case of a single degree of freedom elastic oscillator, the equation of motion taking into account contact phenomena can be written as

$$\ddot{u}(t) + 2\xi_0\omega_0 \cdot \dot{u}(t) + \omega_0^2 \cdot u(t) - (1/m) \cdot W \cdot \lambda(t) = -\ddot{u}_g(t) \quad (5)$$

where m, ξ_0, and ω_0=scalar properties of mass, damping ratio, and angular frequency of the oscillator examined; u denotes its horizontal, relative to the ground, displacement; and u_g=ground displacement. As aforementioned, in the particular case examined herein: $W=-1$.

Contact kinematics for the mechanical configuration of Fig. 1 is described via the simple equation

$$g_N(t) = \delta - u(t) \quad (6)$$

where δ=initial gap or "standoff" distance between the oscillator and the wall. Each time a contact event is detected the pertinent LCPs are solved. For the case of continuous contacts and detachment Eq. (2) takes the form

$$\ddot{g}_N = (1/m)\lambda - [-2\xi_0\omega_0\dot{u} - \omega_0^2 u - \ddot{u}_g(t)],$$
$$\ddot{g}_N \geq 0, \quad \lambda \geq 0, \quad \ddot{g}_N \cdot \lambda = 0 \quad (7)$$

Furthermore for the two phases of impact the two LCPs, Eqs. (3) and (4), specify to

$$\dot{g}_{NC} = \frac{1}{m}\Lambda_{NC} + \dot{g}_{NA}, \quad \dot{g}_{NC} \geq 0, \quad \Lambda_{NC} \geq 0, \quad \dot{g}_{NC} \cdot \Lambda_{NC} = 0 \quad (8)$$

and

$$\dot{g}_{NE} = \frac{1}{m}\Lambda_{NP} + \frac{1}{m}\varepsilon_N\Lambda_{NC} + \dot{g}_{NC},$$
$$\dot{g}_{NE} \geq 0, \quad \Lambda_{NE} \geq 0, \quad \dot{g}_{NE} \cdot \Lambda_{NE} = 0 \quad (9)$$

respectively.

Implementation of Dimensional Analysis

From Eqs. (5)–(9), it becomes evident that the mass of the oscillator, m, can be eliminated from the equations describing the dynamics of the system. This observation is consistent with the implicit assumption of a rigid stationary wall, which presupposes a very large—"infinite"—mass. Indeed, it is intuitively clear that if the mass of the boundary is infinite, then the size of the oscillator's mass drops out of consideration.

Hence, six parameters are required to determine each response quantity of the pounding oscillator (maximum response displacement, $u_{\max}$, velocity, or acceleration): these are the angular frequency, ω_0, and the damping ratio, ξ_0, of the oscillator, the coefficient of restitution, ε_N, and the size of the gap, δ, and the two parameters which describe the predominant pulse, the acceleration "a_p" and the angular frequency of the pulse, $\omega_p=2\pi/T_p$ (see Figs. 1 and 2). Accordingly

$$u_{\max}=f(\omega_0,\xi_0,\delta,\varepsilon_N,a_p,\omega_p) \tag{10}$$

The seven variables appearing in Eq. (10) involve only two reference dimensions, that of length $[L]$ and time $[T]$. According to Buckingham's "Π" theorem the number of independent dimensionless Π products is now (7 variables)$-$(2 reference dimensions)$=5$ Π terms.

When applying the theory of dimensional analysis, there is no restriction in the choice of repeating variables as long as the repeating variables are dimensionally independent (that means that the product of repeating variables cannot be dimensionless). Herein, as in the case of yielding oscillators (Makris and Black 2004a,b; Makris and Psychogios 2006) we select as repeating variables the characteristics of the pulse excitation, α_p and $\omega_p=2\pi/T_p$, since we seek to normalize the nonlinear response including contact, to the energetic length scale of the excitation, $L_e\approx\alpha_p/\omega_p^2=(1/4\pi^2)\alpha_p T_p^2$. Accordingly, Eq. (10) reduces to

$$\frac{u_{\max}\omega_p^2}{a_p}=\phi\left(\frac{\omega_0}{\omega_p},\frac{\delta\omega_p^2}{a_p},\varepsilon_N,\xi_0\right) \tag{11}$$

or

$$\Pi_1=\phi(\Pi_2,\Pi_3,\Pi_4,\Pi_5) \tag{12}$$

with

$$\Pi_1=\frac{u_{\max}\omega_p^2}{a_p},\quad \Pi_2=\frac{\omega_0}{\omega_p},\quad \Pi_3=\frac{\delta\omega_p^2}{a_p},\quad \Pi_4=\varepsilon_N,\quad \Pi_5=\xi_0 \tag{13}$$

The new terms proposed in this paper to characterize structural response of the pounding oscillator are the dimensionless products $\Pi_3=\delta\omega_p^2/a_p$ and $\Pi_4=\varepsilon_N$. The product Π_4 is an obvious choice since it is an already dimensionless parameter with unique significance in impact.

The dimensionless $\Pi_3=\delta\omega_p^2/a_p$ product, though, is a novel proposition which suggests that the size of the gap "δ" can be scaled to the energetic length scale of the excitation (α_p/ω_p^2[m]) rather than scaled to the relative displacement of the adjacent structures when contact of the adjacent structures does not occur ($\chi=\delta/u_{\text{No pounding}}$). The new dimensionless Π_3 product, instead of normalizing the size of the gap with respect to the response without contact (as is done with the "χ" parameter), which uses information from a different problem that requires additional calculations, normalizes the gap (capacity) with a distinct characteristic of the excitation (demand). Thus the description of more involved and realistic systems (multiple adjacent structures) is simplified since Π_3 depends on fewer arguments and, being independent of the dynamical characteristics of the oscillators, can be estimated a priori.

The dimensionless product, $\Pi_2=\omega_0/\omega_p$, is the frequency ratio on which DesRoches and Muthukumar (2002) recently drew attention and identified it as a primary pounding parameter. In summary, the response (displacement) of an elastic oscillator with unilateral contact is fully described by Eq. (12) and the associated dimensionless products given by Eq. (13).

Illustrative Example

To illustrate the underlying mechanism that is based on the persistency of the pulse and the significance of adopting the proposed dimensionless Π terms when examining the pounding oscillator, Fig. 3 plots the response of two different oscillators with different gap distances; when subjected to one-cosine acceleration pulses of different amplitudes, the dimensionless Π products in the two structural systems are the same. What is interesting in Fig. 3 is that the duration of finite contact of the stiff oscillator ($T_0=0.5$ s, $\xi_0=5\%$) is significantly smaller than the duration of finite contact of the more flexible oscillator ($T_0=1.5$ s, $\xi_0=5\%$). Nevertheless, when the response histories of the two oscillators are plotted in dimensionless terms, the two response histories collapse to a single "master" time history. The dimensional analysis presented herein shows clearly that what affects the response is not the size of the gap, δ, but the ratio of the gap to the energetic length scale of the pulse in $\Pi_3=\delta\omega_p^2/a_p$.

The main advantage of the dimensional analysis presented in this paper is that it brings forward the concept of self-similarity—an invariance with respect to changes in scale or size—which is a decisive symmetry that shapes nonlinear behavior. Thus, the response curves, in the proposed dimensionless Π products, for different levels of excitation and a given value of the dimensionless gap ($\Pi_3=\delta\omega_p^2/a_p$) collapse to a single master response history and therefore to single master response spectra (self-similarity). This remarkable property of the dynamic behavior of a pounding oscillator is illustrated in Fig. 4, where the left column plots response spectra in dimensional displacement terms (centimeters) for three different excitation levels and two values of the dimensionless gap, Π_3, and the right column plots the corresponding spectra in the dimensionless Π terms. Note that pertinent conclusions are drawn for excitations without distinct pulse, provided that the appropriate time and length scales are adopted (Dimitrakopoulos et al. 2009a).

Fig. 5 (top) and Fig. 6 (top) plot self-similar response spectra of the pounding oscillator for different values of dimensionless gap $\Pi_3=\delta\omega_p^2/a_p$ and all intensity levels when subjected to a one-sine acceleration pulse (Fig. 5) and a one-cosine acceleration pulse (Fig. 6) that pushes the stationary wall toward (left) and away (right) from the oscillator. For comparison, a more traditional way to interpret the behavior of the pounding oscillator, via the gap ratio parameter "$\chi=\delta/u_{\text{no contact}}$," i.e., the ratio between the gap and the maximum relative displacement of the adjacent structures, if pounding does not occur (e.g., DesRoches and Muthukumar 2002), and the pounding amplification factor "γ," i.e., the maximum response displacement with pounding divided by the corresponding displacement without pounding, is offered in Figs. 5 and 6. For the case of a single pounding oscillator, it turns out that the γ curves shown at the bottom of Figs. 5 and 6 are also self-similar. Nevertheless, when three or more adjacent oscillators are of interest (e.g., Dimitrakopoulos et al. 2009b), multiple χ values emerge and the presentation of the response according to the more traditional way becomes much less direct than the presentation with the dimensionless Π products.

Effect of the Gap Size on the Response

An interesting feature of Figs. 5 and 6 is that the response differs substantially, for small $\Pi_2=\omega_0/\omega_p$ values depending on the directivity of the pulse, meaning whether the pulse pushes the stationary wall toward, or away from, the oscillator. Clearly, in this

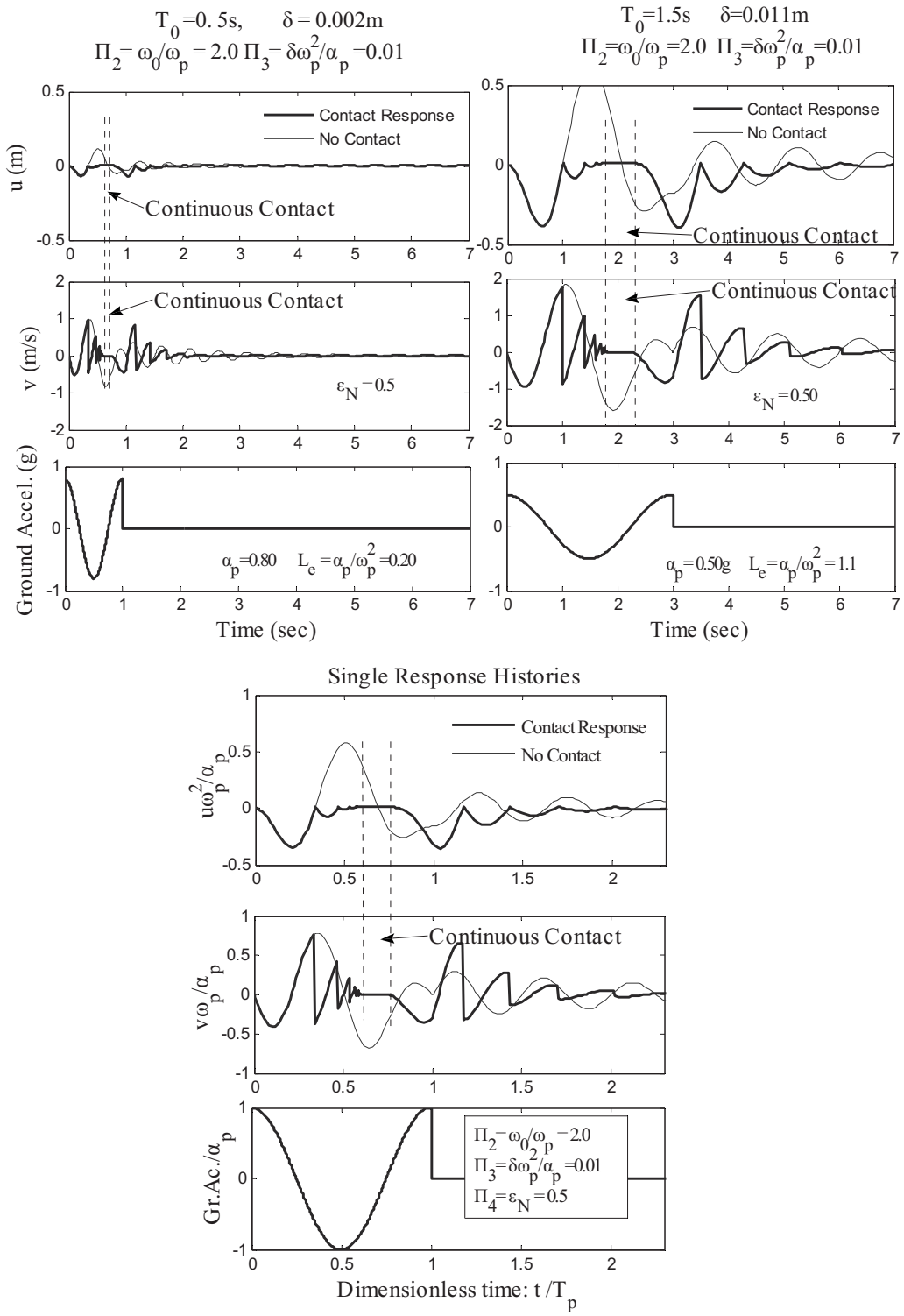

Fig. 3. Top: displacement and velocity histories of pounding oscillators with $T_0=0.5$ s (left) and $T_0=1.5$ s (right) subjected to a one-cosine pulse such that the Π_2 and Π_3 terms are the same. Bottom: response histories above collapse to a single response history when expressed in dimensionless products.

spectral region (of small Π_2 values) the directivity effect governs the response of the system—a characteristic that underlines the asymmetry and the geometrical (boundary) nonlinearity of the problem. This characteristic has received marginal attention with probably the exception of the work of Davis (1992) who suggested that response alters depending on the excitation's directivity, even when steady-state response is concerned (wherein such transient characteristics wear off). In the following, when the pulse is pushing the wall toward the oscillator, it is considered as *normal* pulse; whereas when it is moving the wall away from the oscillator, it is considered as a *reverse* pulse.

According to Figs. 5 and 6 the response is more sensitive to the dimensionless gap value, Π_3, if the directivity of the pulse is reverse rather than normal (Figs. 5 and 6). Special attention de-

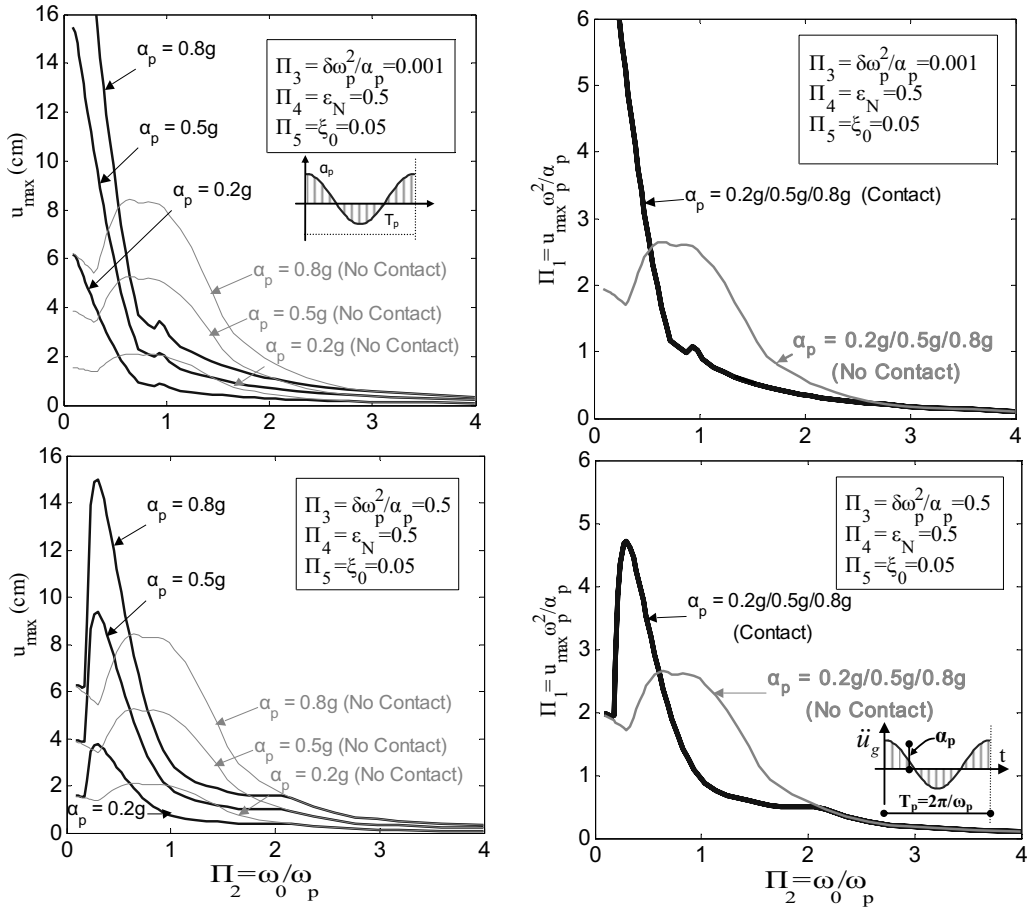

Fig. 4. Left: dimensional displacement spectra of the pounding oscillator subjected to various amplitudes of a one-cosine pulse excitation (self-similarity). Right: all response curves collapse to a single master curve (self-similarity) when plotted in terms of the dimensionless Π products.

serves the intense amplification of the response displacement for small frequency ratios ($\Pi_2=\omega_0/\omega_p$) when the pulse is of normal directivity. This peculiar characteristic of the response, which appears mainly for normal directivity, is explained in the next section, where different response patterns of the pounding oscillator are correlated with distinct spectral regions. It should be noted that generalizing conclusions for the spectral region of very small $\Pi_2=\omega_0/\omega_p$ is precarious since as $\Pi_2\to 0$ (in practice for $\Pi_2 \leq 0.1$) the system is unstable and small perturbations yield unpredictable results.

Regarding the size of the dimensionless gap, Π_3, the most important observation is that the response spectra assume nearly identical values for $\Pi_3 \leq 0.1$, which suggests that the response is insensitive to small values of the dimensionless $\Pi_3=\delta\omega_p^2/a_p$ gap. In fact, the dimensionless response displacement, Π_1, converges to a finite nonzero limit as Π_3 tends to zero; according to the theory of dimensional analysis, one can simply replace Eqs. (11) or Eq. (12) by its limiting expression in which $\Pi_3=0$ [4]

$$\frac{u_{\max}\omega_p^2}{a_p} = \phi\left(\frac{\omega_0}{\omega_p}, 0, \varepsilon_N, \xi_0\right) \tag{14}$$

Accordingly, with this limiting operation the number of arguments in the function $\phi(\,)$ appearing in Eq. (12) reduces further by one argument; it follows that the number of analyses in a parametric study reduces exponentially (Sedov 1959; Barenblatt 1996). Consequently, for small values of δ ($\Pi_3 \leq 0.1$), Eq. (14) reduces to

$$\frac{u_{\max}\omega_p^2}{a_p} = \phi\left(\frac{\omega_0}{\omega_p}, \varepsilon_N, \xi_0\right) \tag{15}$$

The existence of a finite nonzero limit for Π_1 as Π_3 tends to zero indicates that the normalized relative displacement of a pounding oscillator, Π_1, exhibits a complete similarity, or similarity of the first kind (Barenblatt 1996) in the size of the gap, δ, when δ is sufficiently small. Fig. 7 plots contours of $\Pi_3=\delta\omega_p^2/a_p$ on the dimensional (gap δ)—length scale $(1/L_e)$ plane. The energetic length scale, L_e, of the real records shown in Fig. 7 has been based on the acceleration amplitudes, α_p, and angular frequencies, ω_p, reported in Mavroeidis and Papageorgiou (2003). The shaded area under the contour $\Pi_3=0.1$ corresponds to the area where complete similarity prevails. For instance, if δ=1 cm, the response is indifferent whether the oscillator is subjected to the 1978 Tabas earthquake ($1/L_e=1.2$ m^{-1}) or the 1966 Parkfield (C02) earthquake ($1/L_e=5.3$ m^{-1}). Note that typical values for hinge gaps in bridge spans range from 0.6 to 1.3 cm (DesRoches and Muthukumar 2002).

The qualitative characteristics of the pounding oscillator's response can be summarized as follows: regardless whether complete similarity prevails, for small dimensionless gaps ($\Pi_3\to 0$), the response is governed by the successive impacts and is also virtually indifferent to the shape of the pulse, i.e., whether the oscillator is subjected to, e.g., the Tabas or Parkfield earthquakes. This happens since the more flexible the oscillator is, the higher impulse it gains from impact and consequently the longer its re-

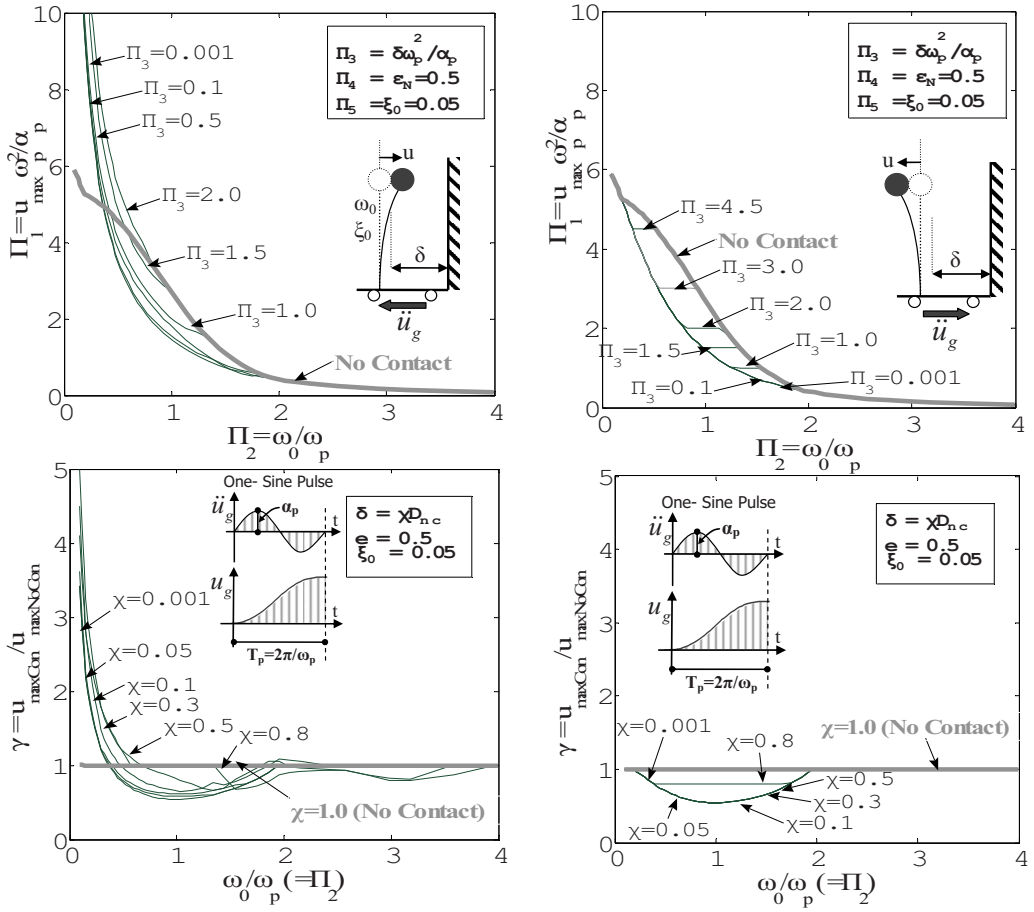

Fig. 5. Self-similar response spectra for the SDOF pounding oscillator excited with a sine pulse, in the proposed dimensionless Π terms (first row) and in the more common terms of amplification factor (second row)

sponse displacement becomes. On the other hand, as the dimensionless gap, Π_3, increases, the structure gains more space to oscillate; thus its "effective" period successively lengthens and the response tends more to the response without contact.

Role of ω_0/ω_p Ratio

Three distinct spectral regions of Π_2 $(=\omega_0/\omega_p=T_p/T_0)$ can be recognized in the response of the single pounding oscillator, regarding the role of unilateral contact on the maximum response displacement (Fig. 8).

1. The first region, for spectral frequencies $\Pi_2=\omega_0/\omega_p<0.5$, wherein the response of the pounding oscillator amplifies due to contact. Additionally, in this region of flexible structures, the directivity of the pulse is of increased importance (Fig. 8). In particular, for both small dimensionless gaps, e.g., $\Pi_3=\delta\omega_p^2/a_p<0.1$, and very small dimensionless spectral frequencies, $\Pi_2=\omega_0/\omega_p<0.1$, the response tends to infinity if the pulse is normal directed (Figs. 5 and 6);
2. In the intermediate region, for $0.5\leq\Pi_2=\omega_0/\omega_p\leq 2.0$, contact systematically deamplifies the maximum response displacement. As the dimensionless Π_3 gap increases, this area shortens, but systematically the highest decrease is observed in the neighborhood of the resonant frequency, $\Pi_2=\omega_0/\omega_p\approx 1$. It is in this limited region that pounding hinders the amplification of the response due to resonance (Priestley et al. 1996) and not throughout the response spectrum as it is often perceived; and
3. In the third region, for $\Pi_2>2$ contact has no significant effect on the response. The oscillator is relatively rigid and either its maximum response displacement is smaller than the gap size ($\Pi_1<\Pi_3$, no contact), or contact occurs but with impact velocities which are too small to alter the response (e.g., the maximum response displacement).

The transition values of Π_2 from one spectral region to the other are a function of the dimensionless $\Pi_3=\delta\omega_p^2/a_p$ gap size, and as Π_3 increases these areas of different behavior converge to the no contact behavior curve. It is interesting that the three spectral regions identified in this work are reminiscent to the spectral regions of the (free standing) elastic oscillator in earthquake engineering (Newmark and Rosenblueth 1971).

The intense amplification of the response for very small Π_2 values ($\Pi_2<0.1$) and its sensitivity to the directivity of the pulse in the same spectral region can be qualitatively explained, considering the limit case of a very flexible oscillator ($T\rightarrow\infty$). When such a system is subjected to a ground motion, its relative to the ground response displacement equals the ground displacement (finite). Yet, if a stationary wall firmly connected to the ground moves toward the still body (normal directivity), an impact takes places and impulse is transferred to flexible oscillator. At the limiting case of $T\rightarrow\infty$ $(K=0)$ the initial velocity leads to endless motion of constant velocity (infinite response displacement). On the contrary, if the stationary wall moves away from the body

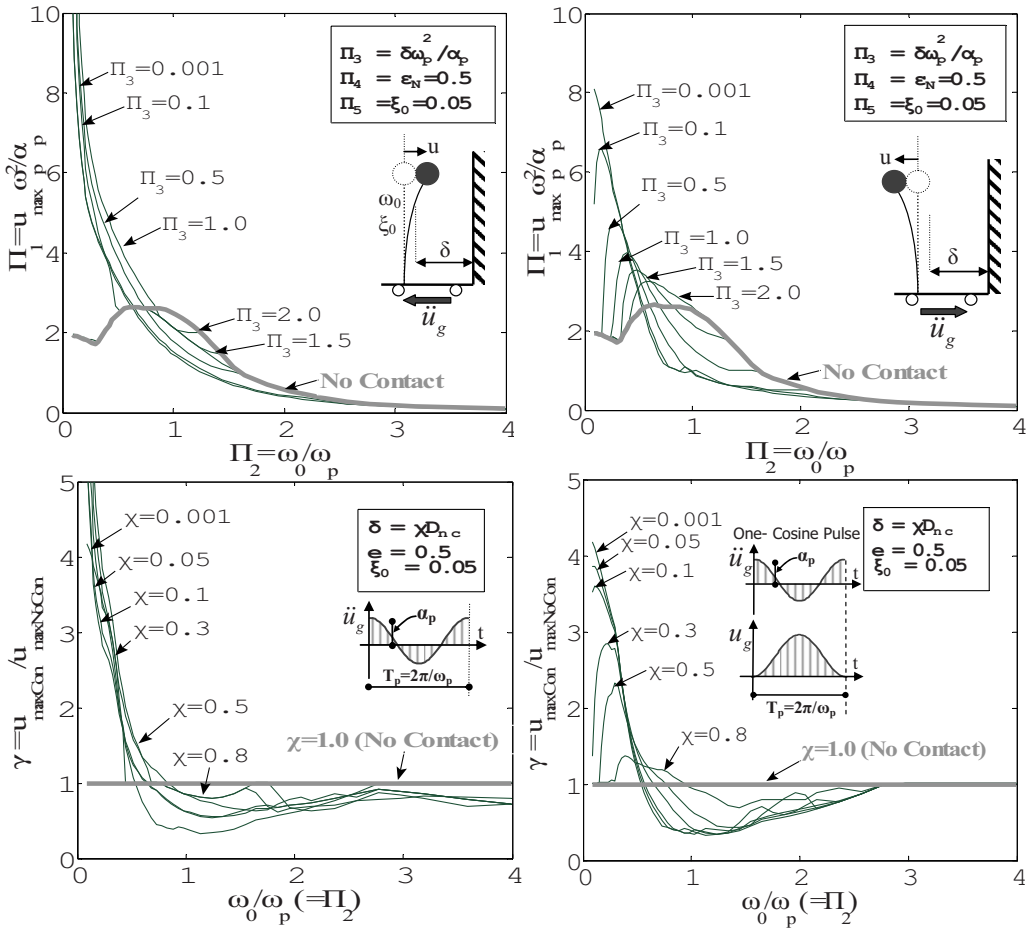

Fig. 6. Self-similar response spectra for the SDOF pounding oscillator excited with a cosine pulse, in the proposed dimensionless Π terms (first row) and in the more common term of amplification factor (second row)

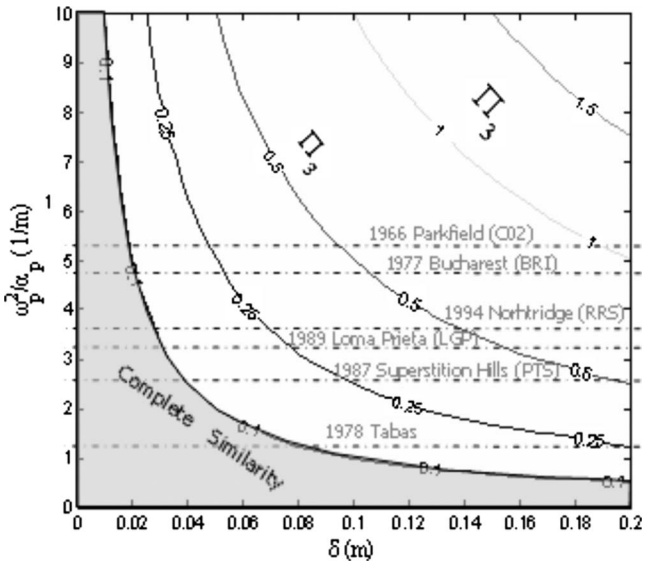

Fig. 7. Contours of the dimensionless gap $\Pi_3=\delta\omega_P^2/\alpha_P$ values for several historic earthquake records. The pulse amplitude and duration are taken from Mavroeidis and Papageorgiou (2003).

(reverse pulse), contact between the boundary and the oscillator does not occur and hence the oscillator remains still. The response of a more realistic long-period structure tends to this limit behavior as its period lengthens. Fig. 9 illustrates the response of such a flexible structure ($T_0=3.0$ s) for different directed pulses.

Effect of the Coefficient of Restitution on the Response

The coefficient of restitution, ε_N, represents the Π_4 term of the functional relationship that governs the maximum response displacement of the pounding oscillator [Eq. (13)] and expresses the inelasticity of impact, with $\varepsilon_N=1$ corresponding to a perfectly elastic impact and $\varepsilon_N=0$ to a perfectly plastic impact. Its influence on the response of the pounding oscillator is schematically presented in Fig. 10 for the whole range of its values: ($\varepsilon_N \in [0,1]$).

It has been stated in the literature (Ruangrassamee and Kawashima 2001) that considering a coefficient of restitution equal to 1, $\varepsilon_N=1$, yields results on the safe side in comparison with smaller coefficients of restitution since during perfectly elastic impacts ($\varepsilon_N=1$) no loss of energy takes place. Nevertheless, the mechanical system of the pounding oscillator is highly nonlinear and the aforementioned argument is false as illustrated in Fig. 10.

This "counterintuitive" behavior is observed for sine pulses of normal directivity, as well as cosine pulses of reverse directivity. It is recalled that cosine acceleration pulses are forward-and-back

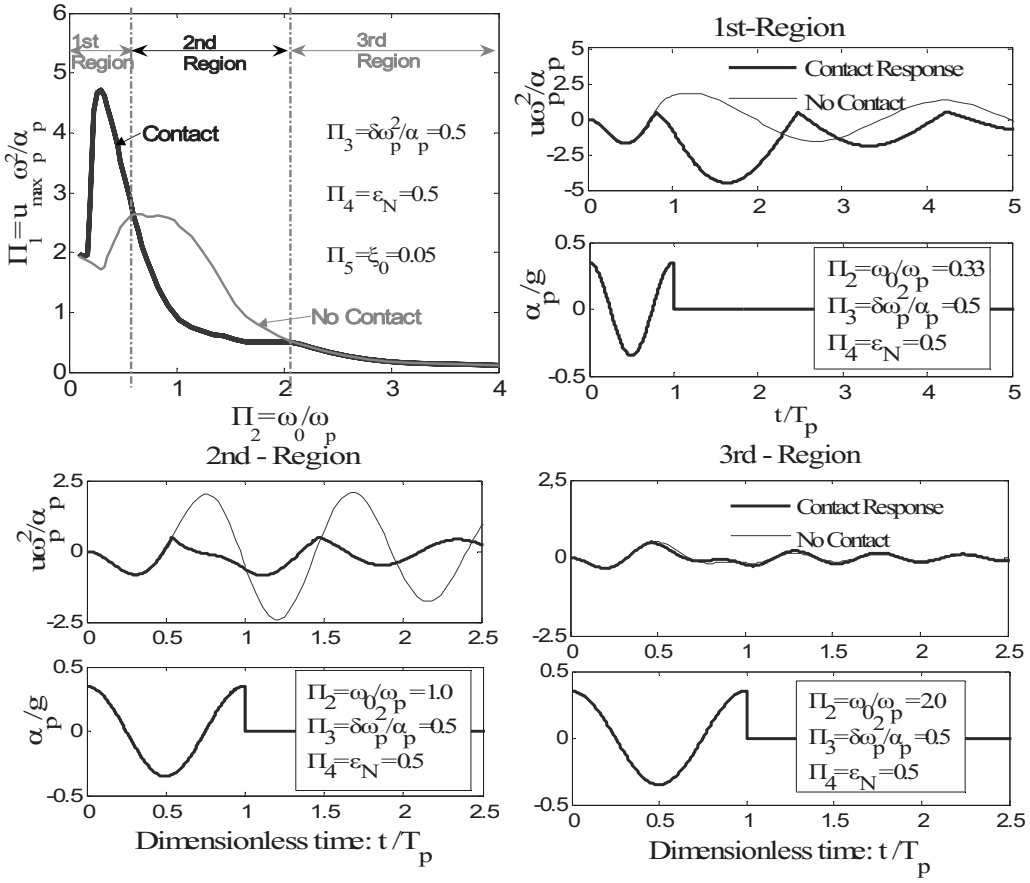

Fig. 8. Time-history response curves for the three distinct spectral regions (Π_2 values) of the SDOF pounding oscillator

displacement movements and thus can be looked upon as a half-cycle reverse and a half-cycle normal directed pulses. Fig. 11 plots two time histories, each for a different coefficient of restitution: $\varepsilon_N=0.2$ for the response in the left column and $\varepsilon_N=1.0$ for the one in the right column, but both for $\Pi_2=\omega_0/\omega_p=1.16$ and a one-cosine excitation pulse of reverse directivity.

It is observed that the higher response displacement results from the smaller coefficient of restitution, $\varepsilon_N=0.2$ (Fig. 11, left). The examination of the velocity plots, second row of Fig. 11, provides the justification for this counterintuitive behavior, which is the smaller coefficient of restitution results in higher energy loss and hence a greater deceleration of the oscillator after impact.

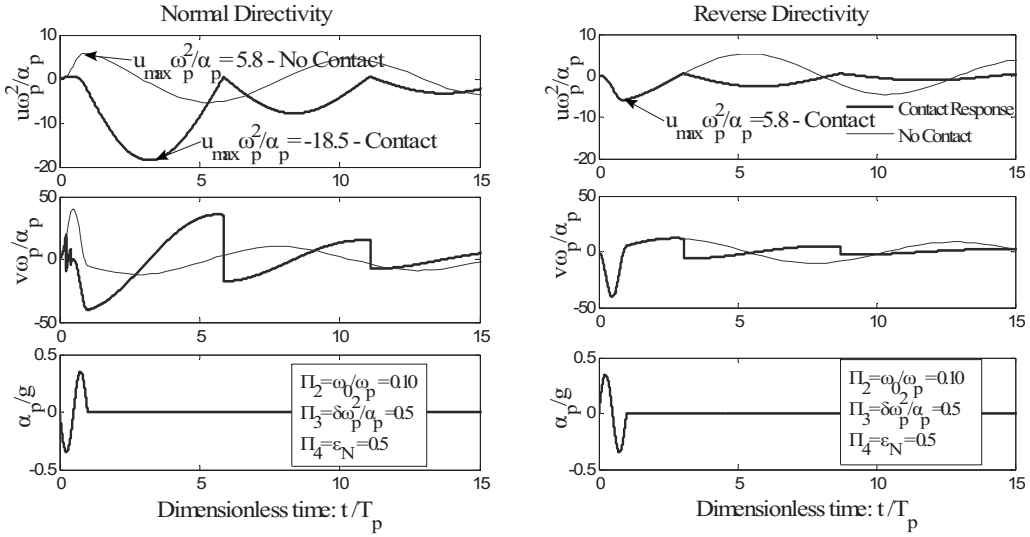

Fig. 9. Very different response time-history displacements of a flexible pounding oscillator ($T_0=3.0$ s, excited by a pulse with duration $T_p=0.30$ s, $\delta=4$ mm) depending on the directivity of the pulse

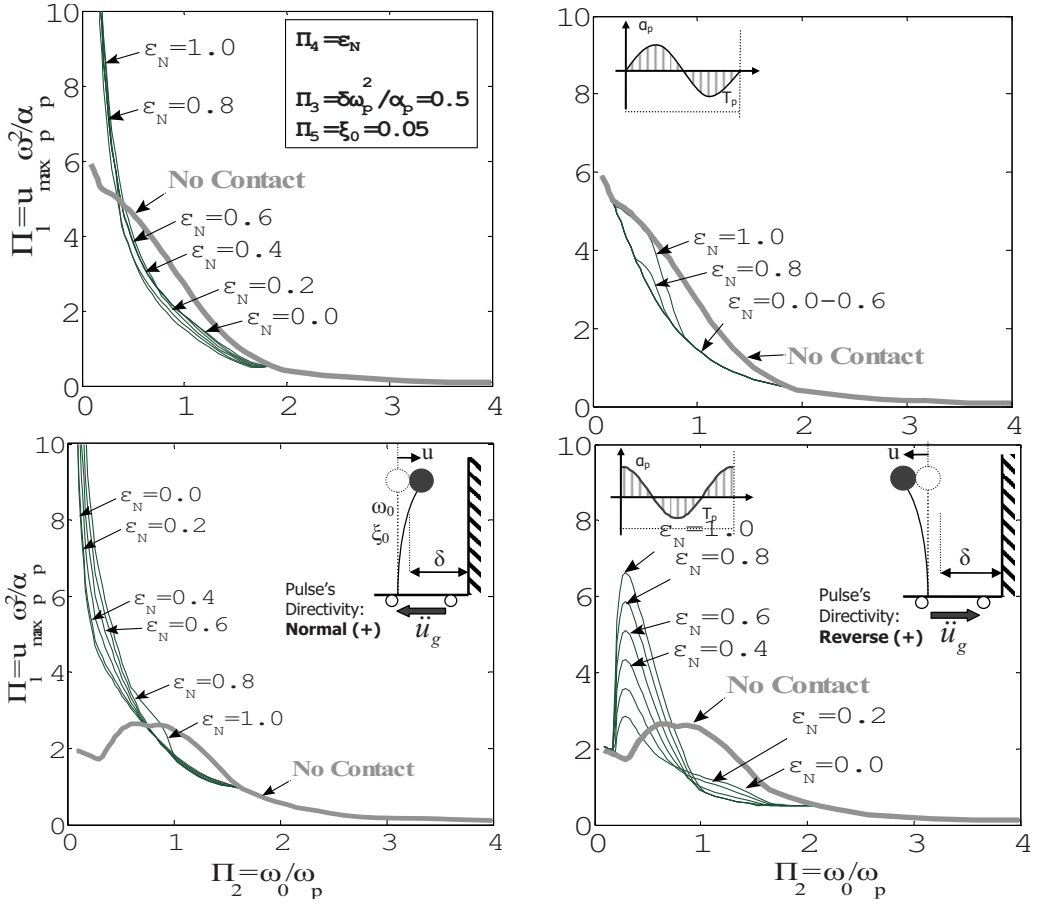

Fig. 10. Self-similar response spectra of the pounding oscillator for the whole range of coefficient of restitution. Rows correspond to different types of excitation pulses and columns to normal (left) and reverse (right) directivity.

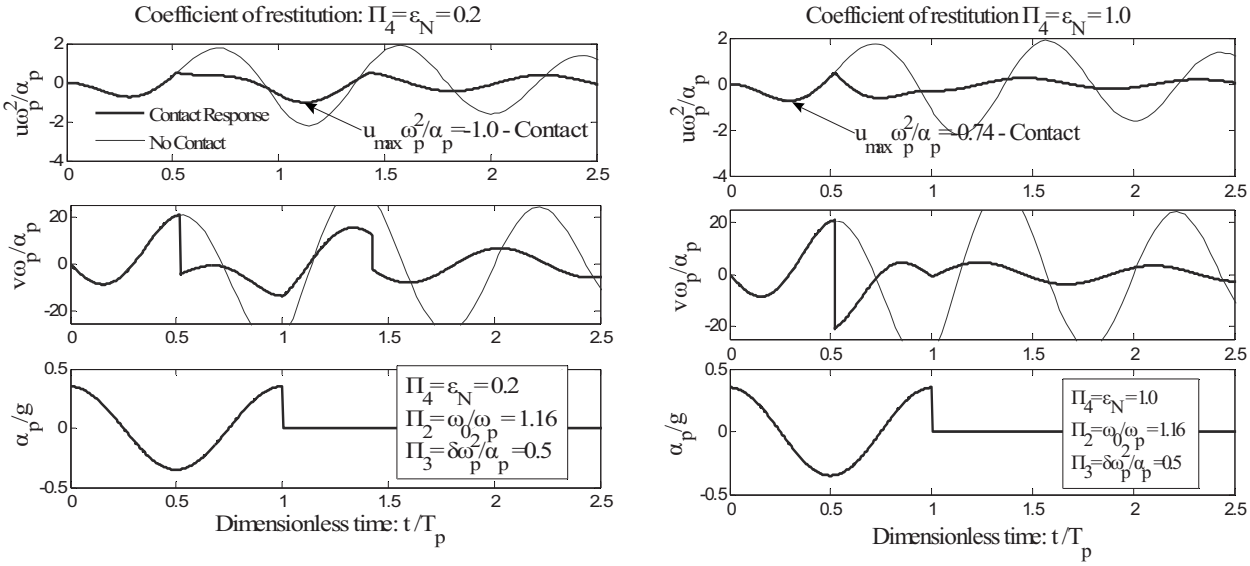

Fig. 11. Counterintuitive behavior of the pounding oscillator: left column plots the response for a small coefficient of restitution: ε_N=0.2, yet the response displacement is higher than for a coefficient of restitution: ε_N=1.0 (*elastic impact*—right column). Second row illustrates the dimensionless velocity time histories.

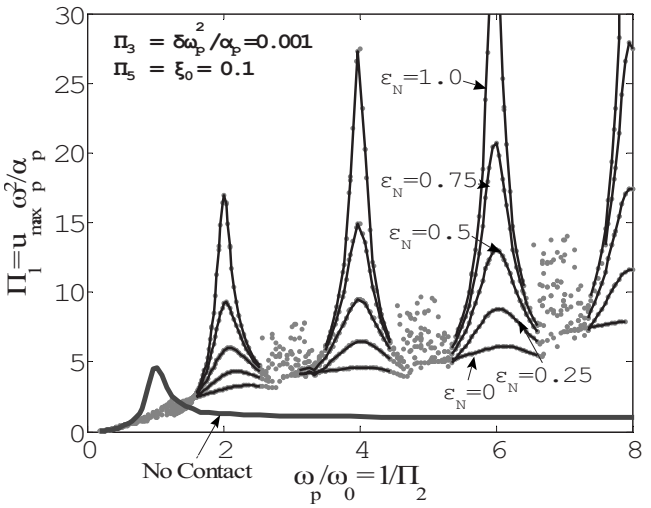

Fig. 12. Steady-state response under harmonic excitation in the dimensionless Π terms for zero gap conditions ($\Pi_3 \approx 0$) and several coefficient of restitutions ($\varepsilon_N = \Pi_4$)

As a further consequence, when the ground excitation changes sign (reverses), the oscillator is accelerated more drastically, thus exhibiting longer response displacements. Similar counterintuitive responses which are also due to the accelerating and decelerating sequents of the pulses have been identified by Makris and Roussos (2000) when studying the rocking response of rigid structures.

Steady-State Response under Harmonic Excitation

Lastly, the steady-state response under harmonic excitation is also revisited herein since, on one hand, it provides useful insight into the dynamic behavior of the pounding oscillator and, on the other hand, it serves as a connecting link between our work and that of previous researchers. It is reminded that herein a nonsmooth approach is adapted to model contact, while in the studies referenced (Wolf and Skrikerud 1980; Shaw and Holmes 1983; Davis 1992; Thompson and Stewart 2001) impact is simulated via a contact element approach.

Fig. 12 plots the maximum response displacement, dimensionless Π_1 term, under harmonic excitation for zero gap conditions, $\Pi_3 = 0.001$, and given values of the coefficient of restitution. As it is well known, due to the repeated poundings, the natural frequency of the oscillator is not damped out entirely as the excitation insists (elastic—no contact response), but it results in periodic responses with lower frequencies than the natural one, called subharmonics (Thompson and Stewart 2001). These subharmonic resonances accentuate the response for integer values of the natural frequency (e.g., the corresponding peaks for $1/\Pi_2 \approx 2,4,6,8$) as marked also by Wolf and Skrikerud (1980) and Thompson and Stewart (2001). Between successive subharmonic resonances, there exist regions of chaotic response in accordance with Davis (1992).

The most important observation, from the standpoint of earthquake engineering though, is the little resemblance the steady-state response for harmonic excitation (Fig. 12) bears with the transient response for typical pulses (Fig. 5, 6, and 10) which are a more realistic approximation of an earthquake excitation.

Conclusions

In this paper the response of a SDOF oscillator pounding against a stationary monolithic wall is revisited using the theory of dimensional analysis. The application of the proposed method hinges upon the existence of a distinct time scale and a length scale that characterize the most energetic component of ground shaking. Such time and length scales emerge naturally from the distinguishable pulses which dominate a broad class of strong earthquake records; they are directly related with the rise time and slip velocity of faulting and can be formally extracted with validated mathematical models published in the literature.

The proposed dimensionless Π products reduce the number of variables in this problem by 2 and are liberated from the need to calculate the response of the SDOF oscillator without pounding. The proposed dimensional analysis unveils the symmetry of self-similarity and when the response is presented in terms of the dimensionless Π products, all response curves collapse to a single master curve. This remarkable behavior is true despite the realization of contacts with increasing durations as the excitation level increases.

The dimensional analysis presented in this work shows that what really matters during the phenomenon of pounding is not the size of the gap, δ, alone but its normalized value, with respect to the energetic length scale of the excitation $L_e = \alpha_p/\omega_p^2$. Furthermore, when the value of the dimensionless gap, $\Pi_3 = \delta\omega_p^2/\alpha_p$, is small (say $\Pi_3 < 0.1$), the normalized displacement, $\Pi_1 = u_{max}\omega_p^2/\alpha_p$, is merely independent of Π_3 or in mathematical terms the dimensionless displacement Π_1 exhibits a complete similarity, or similarity of the first kind in the normalized gap, Π_3.

The condensation of the parametric analysis that was made possible from the dimensional analysis sheds light on the sensitivity of the response depending whether the stationary wall is moving toward or away from the oscillator; it was shown that when $\Pi_2 = \omega_0/\omega_p$ is small, the response is most sensitive to the directivity of the pulse.

Our analysis concludes that the response of the pounding oscillator is characterized by three main spectral areas: (1) the area of small $\Pi_2 = \omega_0/\omega_p$ (say $\Pi_2 < 0.5$—flexible structures or short pulses) where the response of the pounding oscillator amplifies and far exceeds the response of the oscillator without pounding; (2) the area of intermediate values of Π_2 (say $0.5 \le \omega_0/\omega_p \le 2$—"resonance") in which the response of the pounding oscillator deamplifies and is smaller than the response of the oscillator without pounding; and (3) the area of large $\Pi_2 = \omega_0/\omega_p$ (say $\Pi_2 > 2$; stiff structures or long duration pulses) in which pounding is immaterial.

Finally the study depicts counterintuitive trends in the response of the pounding oscillator, wherein smaller coefficients of restitution yield higher maximum response displacements. These counterintuitive trends are shown to arise from the accelerating and decelerating sequents of the excitation pulses.

Acknowledgments

Partial financial support to the first writer was provided by the Marie Curie fellowship (Grant No. HPMT-GH-01-00359-16).

References

Aki, K. (1983). "Strong-motion seismology in earthquakes: Observation, theory and interpretation." *Proc., Int. School of Physics*, H. Kanamori

and E. Boschi, eds., North-Holland, Amsterdam, The Netherlands, 223–250.
Alavi, B., and Krawinkler, H. (2004). "Behavior of moment-resisting frame structures subjected to near-fault ground motions." *Earthquake Eng. Struct. Dyn.*, 33(6), 687–706.
Barenblatt, G. I. (1996). *Scaling, self-similarity, and intermediate asymptotics*, Cambridge University Press, Cambridge, U.K.
Brogliato, B. (1999). *Nonsmooth mechanics*, 2nd Ed., Springer, Berlin.
Brune, J. N. (1970). "Tectonic stress and the spectra of seismic shear waves from earthquakes." *J. Geophys. Res.*, 75, 4997–5009.
Davis, R. O. (1992). "Pounding of buildings modeled by an impact oscillator." *Earthquake Eng. Struct. Dyn.*, 21, 253–274.
DesRoches, R., and Muthukumar, S. (2002). "Effect of pounding and restrainers on seismic response of multiple-frame bridges." *J. Struct. Eng.*, 128(7), 860–869.
Dimitrakopoulos, E. G., Kappos, A. J., and Makris, N. (2009a). "Dimensional analysis of yielding and pounding structures for records without distinct pulses." *Soil. Dyn. Earthquake Eng.*, 29(7), 1170–1180.
Dimitrakopoulos, E. G., Makris, N., and Kappos, A. J. (2009b). "Dimensional analysis of the earthquake-induced pounding between adjacent structures." *Earthquake Eng. Struct. Dyn.*, 38(7), 867–886.
Hall, J. F., Heaton, T. H., Halling, M. W., and Wald, D. J. (1995). "Near-source ground motion and its effects on flexible buildings." *Earthquake Spectra*, 11(4), 569–605.
Heaton, T. H., Hall, J. F., Wald, D. J., and Halling, M. W. (1995). "Response of high-rise and base-isolated buildings to a hypothetical Mw 7.0 blind thrust earthquake." *Science*, 267, 206–211.
Langhaar, H. L. (1951). *Dimensional methods and theory of model*, Wiley, New York.
Leine, R. I., van Campen, D. H., and Glocker, C. (2003). "Nonlinear dynamics and modeling of various wooden toys with impact and friction." *J. Vib. Control*, 9, 25–78.
Makris, N. (1997). "Rigidity–plasticity–viscosity: Can electrorheological dampers protect base-isolated structures from near-source ground motions?" *Earthquake Eng. Struct. Dyn.*, 26, 571–591.
Makris, N., and Black, C. J. (2004a). "Dimensional analysis of rigid-plastic and elastoplastic structures under pulse-type excitations." *J. Eng. Mech.*, 130(9), 1006–1018.
Makris, N., and Black, C. J. (2004b). "Dimensional analysis of bilinear oscillators under pulse-type excitations." *J. Eng. Mech.*, 130(9), 1019–1031.
Makris, N., and Black, C. J. (2004c). "Evaluation of peak ground velocity as a "good" intensity measure for near-source ground motions." *J. Eng. Mech.*, 130(9), 1032–1044.
Makris, N., and Chang, S. (2000). "Effect of viscous, visco-plastic and friction damping on the response of seismic isolated structures." *Earthquake Eng. Struct. Dyn.*, 29, 85–107.
Makris, N., and Psychogios, C. (2006). "Dimensional response analysis of yielding structures with first-mode dominated response." *Earthquake Eng. Struct. Dyn.*, 35, 1203–1224.
Makris, N., and Roussos, Y. (2000). "Rocking response of rigid blocks under near-source ground motions." *Geotechnique*, 50(3), 243–262.
Mavroeidis, G. P., and Papageorgiou, A. S. (2003). "A mathematical representation of near-fault ground motions." *Bull. Seismol. Soc. Am.*, 93(3), 1099–1131.
Newmark, N. M., and Rosenblueth, E. (1971). *Fundamentals of earthquake engineering*, Prentice-Hall, Upper Saddle River, N.J.
Papageorgiou, A. S., and Aki, K. (1983). "A specific barrier model for the quantitative description of inhomogeneous faulting and the prediction of strong ground motion II: Applications of the model." *Bull. Seismol. Soc. Am.*, 73, 953–978.
Pfeiffer, F., and Glocker, C. (1996). *Multibody dynamics with unilateral contacts*, Wiley, New York.
Priestley, M. J. N., Seible, F., and Calvi, G. M. (1996). *Seismic design and retrofit of bridges*, Wiley, New York.
Ruangrassamee, A., and Kawashima, K. (2001). "Relative displacement response spectra with pounding effect." *Earthquake Eng. Struct. Dyn.*, 30, 1511–1538.
Sedov, L. I. (1959). *Similarity and dimensional methods of mechanic*, Academic, San Diego.
Shaw, S. W., and Holmes, P. J. (1983). "A periodically forced piecewise linear oscillator." *J. Sound Vib.*, 90(1), 129–155.
Thompson, J. M. T., and Stewart, H. B. (2001). *Nonlinear dynamics and chaos*, 2nd Ed., Wiley, New York.
Veletsos, A. S., Newmark, N. M., and Chelepati, C. V. (1965). "Deformation spectra for elastic and elastoplastic systems subjected to ground shock and earthquake motions." *Proc., 3rd World Conf. on Earthquake Engineering*, Vol. 2, Wellington, New Zealand, 663–682.
Wolf, J. P., and Skrikerud, P. E. (1980). "Mutual pounding of adjacent structures during earthquakes." *Nucl. Eng. Des.*, 57, 253–275.